UV-LASER INDUCED SURFACE REACTION
- DESORPTION AND ETCHING -

Yoshitada Murata

Institute for Solid State Physics, The University of Tokyo

Roppongi 7-221, Minato-ku, Tokyo 106, Japan

ABSTRACT

Photostimulated desorption of NO chemisorbed on Pt(001) at 80K has been studied by the (1+ 1)-resonance-enhanced multiphoton ionization ((1+1)-REMPI) technique. A linearly polarized ArF excimer laser (λ=193 nm ,6.41eV) is used as the pump laser. A high adsorption rate selectivity was found in the exposure dependence of the NO desorption yield. The NO desorption yield increases drastically when the amount of NO exposure exceeds ~1.8 L. This result shows that the amount of NO species with a large cross section for photostimulated desoption increases drastically at higher NO coverages.

Using scanning tunneling microscopy, we have observed structural modifications of the chlorinated Si(111)-7x7 surface induced by 266nm laser irradiation. At very low laser fluence of $0.7mJ/cm^2$, at which thermal desorption can be ignored, a periodic striped pattern of a single domain is imaged. This pattern consists of flat terraces and narrow grooves of ~60 and ~10A in width, respectively.

DESORPTION ON Pt(001)-NO

Laser has developed into a useful excitation source for desorption studies

because of the advantages auch as high photon flux, high directivity, high mono-

chromaticity, and short pulse duration. For molecules chamisorbed on well-

defined metal surfaces, however, there have been only a few studies on laser

stimulated desorption induced by electronic excitations, partly because thermal

processes often dominate over photochemical processes, and partly because

deexcitation of molecules proceeds rapidly on metal. Recently, we have reported ultraviolet-laser stimulated desorption studies of NO chemisorbed on Pt(001) and the laser fluence dependence of the desorption yield, the translational and internal energy distributions of desorbed NO, and the desorption cross sections were measured.[1-2] All of the results support that desorption of chemisorbed NO is induced by electronic excitations. In the present study, we report an advanced study of ultraviolet-laser stimulated desorption of NO chemisorbed on Pt(001) mainly concerned with the adsorption state selectivity.

An ArF excimer laser was linearly polarized with a polarizer (Showa Koki). The polarized laser impinged on the Pt(001) surface at 81° from the surface normal. The desorbed NO molecules in the ground state were ionized with the probe laser via the (1 + 1)-REMPI process, and detected with a microchannel plate assembly. The second harmonic of a tunable Coumarin 460 dye laser was used as the probe laser. Surface cleaning, characterization, and photostimulated desorption measurements were carried out in an ultrahigh-vacuum(UHV) chamber equipped with low-energy electron diffraction(LEED) and Auger electron spectroscopy optics.

Figure 1 shows the LEED pattrns of a Pt(001) surface after various NO exposures at 80K. A clean Pt(001) surface exhibited a (20 x 5)-like LEED pattern (Fig.1(a)). The clean Pt(001)-(20 x 5) surface was reported to have a structure that the topmost Pt layer is hexagonally reconstructed with a rotation angle of 0.7° . An NO-saturated Pt(001) surface exhibited a diffuse (20 x 5) pattern with enhanced (1 x 1) spots and high background intensity (Fig.1(b)). This result indicates that some portion of the NO-saturated Pt(001) surface is transformed to the (1 x 1) structure, while the rest remains reconstructed. The enhancement

of the (1 x 1) spots, however, was observed to occur suddenly in a narrow NO exposure range of 0.8 – 1.0 L (1L = 1×10^{-5} Torr.s) (Fig.1(c) and (d)). The LEED pattern remained unchanged for increasing NO exposure, except for the increase of background intensity.

Figure 2 shows the decays of the NO desorption yield against a sequence of the p-polarized pump laser irradiation. Before every measurement, the Pt(001) -(20 x 5) clean surface was exposed to NO at 80K, and the residual NO gas was quickly pumped out. The probe laser wavelength was fixed at the band edge of the $P_{21}+Q_{11}$ branch, i.e., NO in the $X^2O_{1/2}(v=p, j=1/2\sim9/2)$ states was probed. Fluences of the pump and the probe laser were 1.0 and 3.2 mJ/cm^2, respectively. The NO desorption yield was found to increase drastically when the amount of NO exposure exceeds $\sim$1.8L. The decays of the NO desorption yield (Y (N)) were fitted by a curve composed of two exponential components on the basis of the least-squares method;

$$Y(N) = I_1 \exp(-\sigma_1 N) + I_2 \exp(-\sigma_2 N) \dots\dots\dots\dots\dots\dots\dots\dots\dots (1)$$

where N is the pump laser shot number. The subscripts 1 and 2 represent the fast and slow exponential components, respectively. The double exponential decay suggests that there are at least two NO species sensitive to photostimulasted desorption. The relative total desorption amount of a specific NO specices A is given by:

$$A = I_i / \sigma_i \dots\dots\dots\dots\dots\dots\dots\dots\dots\dots\dots\dots\dots\dots\dots\dots (2)$$

The desorption cross section σ_{di} (cm^2) is given by :

$$\sigma_{di} = \sigma_i / \phi \dots\dots\dots\dots\dots\dots\dots\dots\dots\dots\dots\dots\dots\dots\dots (3)$$

where ϕ is the photon flux density per one laser shot (photons/cm^2). The values of A_i and σ_{di} are listed in Table I. The fast and slow decay components

give the desorption cross sections of $(4\pm1)\text{x}10^{-18}$ and $(8\pm2)\text{x}10^{-20}$ cm^2, respectively. The fast decay component is probably derived from NO adsorbed on minor defect sites, because the total desorption amount for this component is two orders of magnitude smaller than that for the slow exponential decay component of the decay after NO exposure of 5.2 L.

The relative total desorption amount for the slow decay component was found to increase drastically when the amount of NO exposure exceeds ~1.8 L (see Table I). This result suggests that the ammount of the NO species responsible for the slow decay component increases drastically above the 1.8 L exposure.   According to a vibrational spectroscopic study by. Gardner et al. using IRAS, three chemisorbed NO species are supposed to be present on a Pt(001) surface at 80K.   The first is NO at an on-top site in the   reconstructed Pt-(20 x 5) area (N-O stretching frequency (ν_{N-O}) = 1680~1700 cm^{-1}), and the second is NO at a site between on-top and bridge positions in the Pt-(1 x 1) area (ν_{N-O} = 1630~1640 cm^{-1}).   The first and the second NO species were reported to be present before and after the (20 x 5)→(1 x 1) structural transformation of the top-most Pt layer at 90K, respectively.   The third NO specieswas observed for an NO-saturated Pt(001) surface at 90K (ν_{N-O} = 1700~1820 cm^{-1}).   Gardner et al. assigned it to NO adsorbed at defect sites created by the (20 x 5)→ (1 x 1) structural transformation of the top-most Pt layer, because the N-O stretching band for the third NO species was found to be broad.

The present LEED observations show that the (20 x 5)→(1 x 1) structural transformation of the top-most Pt layer occurs in the NO exposure range of 0.8-1.0L (see Fig. 1(c) and (d)). The NO desorption yield under pump laser irradiation, however, was little for NO exposures up to 1.4L (see Fig. 2 and Table I).

This result suggests that the first as well as the second NO species are not so sensitive for photostimulated desorption. The NO desorption yield, on the other hand, was found to increase drastically when the amount of NO exposure exceeds ~1.8 L. This result suggests that the third NO species is most sensitive for photostimulated desorption.

ETCHING ON Si(111)-Cℓ

We have studied ultraviolet(UV)-laser-induced etching on the Si(111)-7x7 surface saturated with chlorine by using scanning tunneling microscopy(STM) for the surface structure observation. STM images were observed after irradiation with very low laser fluence in ultrahigh vacuum (UHV), in order to eliminate both the ambient gas effect and the thermal processes. The structure was clearly changed before and after only 600 shots irradiation at 266 nm with laser fluence of ~0.7 mJ/cm^2.

Figure 3 shows an STM topograph of the chlorinated surface at the saturation coverage before laser irradiation at a sample bias of +3 V (empty state). The troughs based on the dimer rows described in the dimer-adatom-stacking-fault (DAS) model are clearly seen in the figure. Formation of SiCl$_2$ and SiCl$_3$ species at higher-coverage area is suggested, since some of the Cl atoms are arranged out of the registry with the on-top site of adatoms. Figure 4 shows an STM topograph at a sample bias of +3 V after laser irradiation. The surface structure is obviously changed by laser irradiation and a periodic striped pattern is found. Parallel grooves with ~10 A in width run on the surface at nearly equal distances of ~60 A and along the direction parallel to the boundary between the faulted- and the unfaulted-half in the DAS model of the Si

(111)-7x7 surface. The pattern is a single domain in spite of three-fold symmetry of the Si(111)-7x7, surface geometry. The direction of the polarity of the s-polarized laser on the surface was perpendicular to the grooves. However, it is indefinite whether the groove direction correlates with the laser polarity or not.

Figure 5 shows an STM topograph at a sample bias of +1 V on the Si(111) surface, which was obtained by annealing the chlorine-saturated Si(111)-7x7 surface at 400°C for 5 min. An atomic resolution topograph shows the flat rest-atom layer with 42 surface atoms in the 7x7 unit mesh. Which are consistent with the second layer of the DAS model. The surface modification with 470°C annealing has been already demonstrated by Villarrubia and Boland, but we performed similar experiments for comparing it with the present experimental results. The thermally modified surface shown in Fig. 5 is isotropic and clearly different from the UV-laser etching surface shown in Fig. 4. So, the surface modification with the striped pattern is concluded to be caused by photo-etching due to the non-thermal process.

The etching mechanism in these surface modifications is not so simple that we cannot elucidate the formation mechanism in the present stage. It is considered, however, that surface diffusion of chlorine atoms plays an imporatnt role in the groove formation. The following model can be speculated with the aid of other experimental results. Desorption of only the $SiCl_2$ and/or $SiCl_3$ species is induced by valence electron exciation due to UV-laser irradiation. The rest-atom layer is formed in the region where the backbond breaking has occurred, and the chlorinated adatom layer remains in a terrace area at which Cl atoms are adsorbed on the on-top site of the adatoms. The preferred photo-

etching occurs at defect sites such as a terminal point of the grooves after the diffusion of Cl atoms there, since the $SiCl_2$ species are easily formed due to the backbond breaking at defect sites and desorbed by the photochemical process. Then, the striped pattern is built up in UV-laser etching induced by valence electron excitation.

REFERENCES

1. K. Mase, S. Mizuno, M. Yamada, I. Doi, T. Katsumi, S. Watanabe, Y. Achiba, and Y. Murata, J. Chem. Phys. 91, 590 (1989).

2. K. Mase, S. Mizuno, Y. Achiba, and Y. Murata, Rev. Solid State Sci. 4, 721 (1990).

3. K. Mase, S. Mizuno, Y. Achiba, and Y. Murata, Surf. Sci. 242, 444 (1991).

TABLE I. The desorption cross sections (σ_{di}) and the relative total desorption amounts (A_i) for the NO desorption yield decays after various NO exposures. The subscripts 1 and 2 represent the fast and slow decay components, respectively.

Exposure [L]	A_1 (x10⁵)	σ_{d1} [cm²]	A_2 (x10⁵)	σ_{d2} [cm²]
0.30	1.5	4.1×10^{-19}	14	8.2×10^{-21}
1.40	2.7	4.6×10^{-19}	24	9.8×10^{-21}
1.79	2.5	3.7×10^{-19}	128	6.2×10^{-22}
5.2	2.7	3.3×10^{-19}	202	7.0×10^{-22}

Fig. 1. LEED patterns of a Pt(001)-(20x5) surface after various NO exposures at 80 K; (a) a clean surface, (b) 7.9 L, (c) 0.91 L, (d) 5.81 L.
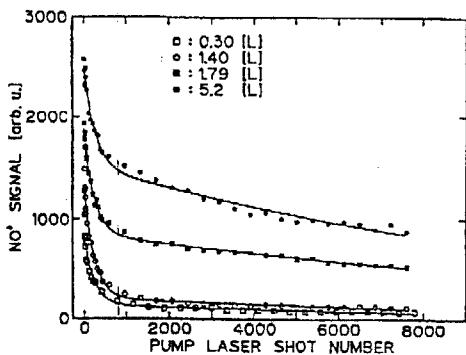

Fig. 2. Decays of the NO desorption yield against a sequence of the p-polarized pump laser irradiation. The decays were slightly distorted by the drift of the probe laser wavelength. The solid lines are the fit curves composed of the fast and slow decay components.
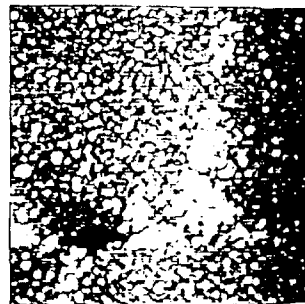

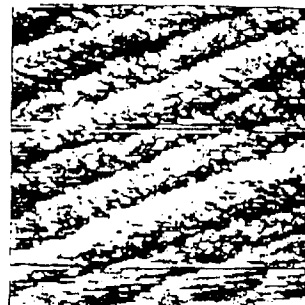Fig. 3. STM image of the Cl-saturated Si(111)-7x7 surface at a sample bias of +3 V. The area shown is 450x450 Å².

Fig. 4. STM image of the Cl-saturated Si(111)-7x7 surface following 268 nm laser etching with 600 shots. Laser fluence is 9.7 mJ/cm². The image is recorded at...
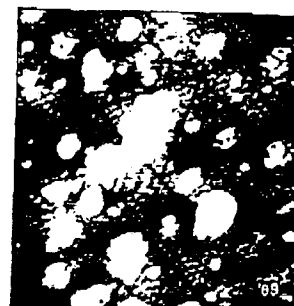

Fig. 5. STM image of the Cl-saturated Si(111)-7x7 surface following an annealing at 400·C for 5 min. The image is recorded at a sample bias of +1 V and the area shown is 155x155 A².